

Gurpreet Kaur Gulati¹, Bharath Srivathsan¹, Alessandro Cerè¹, Chng Mei Yuen Brenda¹, Dzmitry Matsukevich^{1,2} and Christian Kurtsiefer^{1,2}

¹Centre for Quantum Technologies, National University of Singapore, Singapore 117543

²Department of Physics, National University of Singapore, Singapore 117542

We present a source of photon pairs based on a four-wave mixing process in a cold ensemble of Rubidium 87 atoms that exploit a cascade decay scheme, similar to the one proposed by [1]. Here we present a characterization of the generated photon pairs bandwidth and polarization correlation. We also explore the rich structure offered by the hyperfine splitting of the intermediate energy level to observe quantum beats, a signature of the non-classicality of the pair generation process.

Non-collinear setup

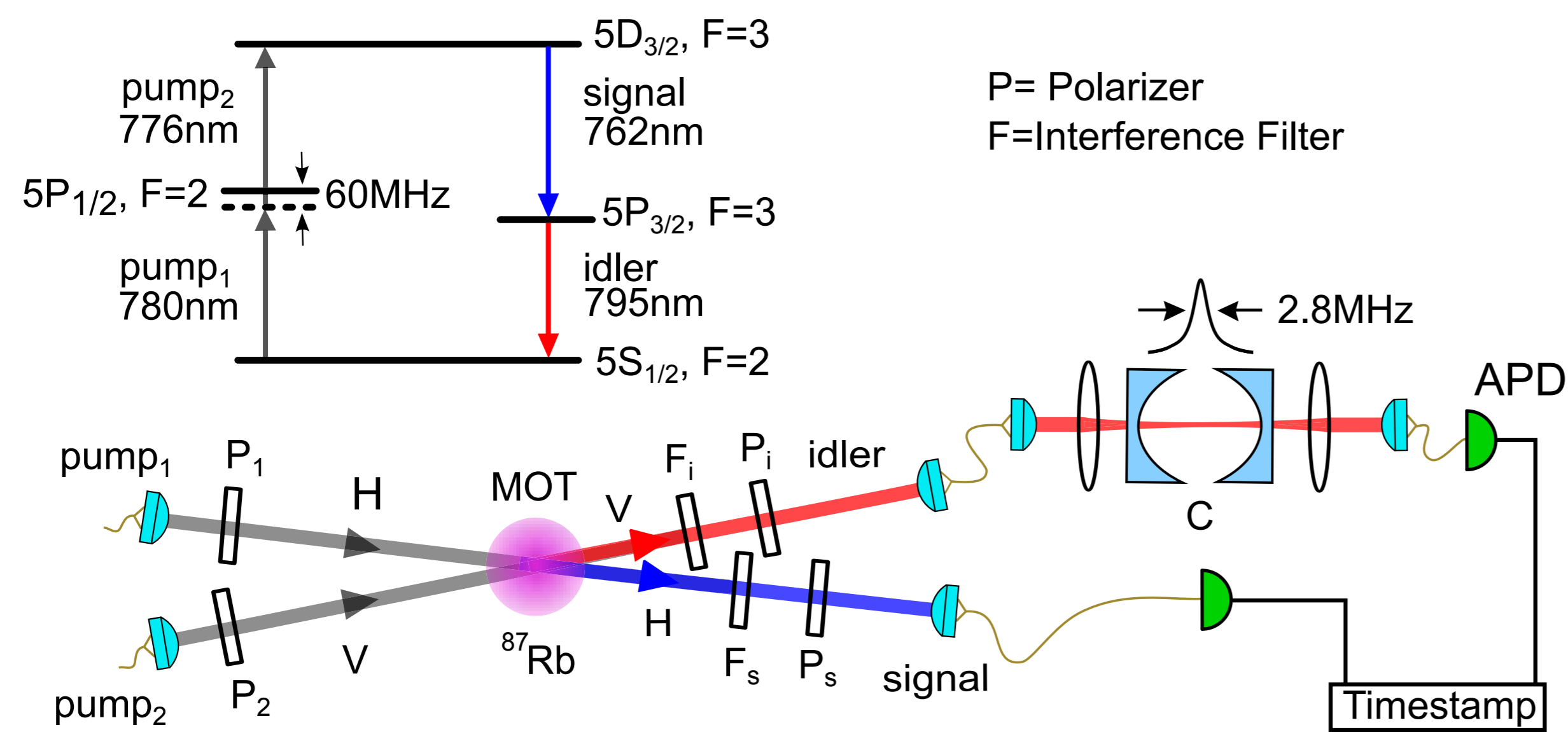


FIGURE 1: Setup of the source. In the first realization we used a non-collinear geometry for the pumps, signal, and idler beams. In the inset, the cascade level scheme used.

Pair correlation

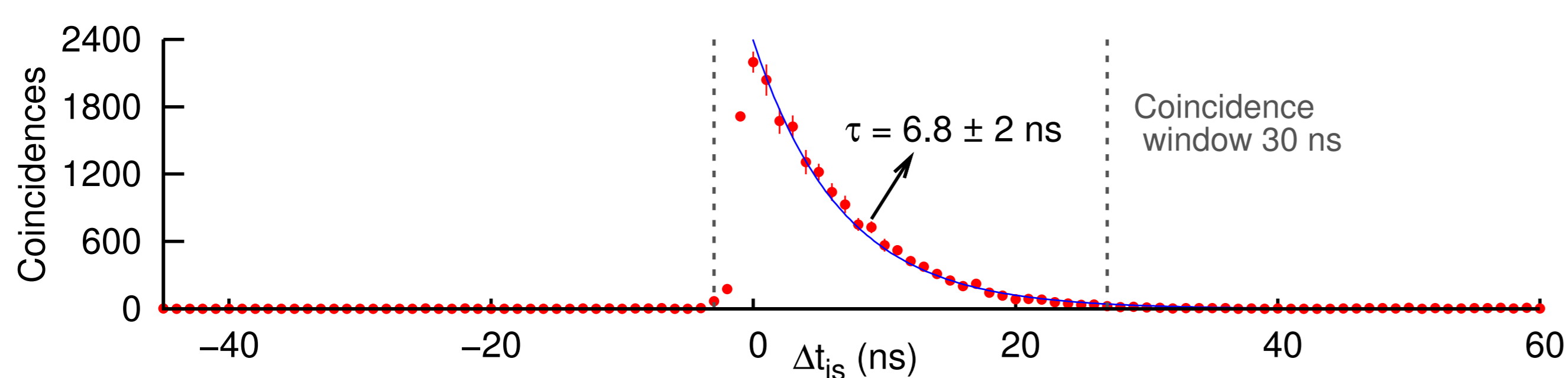


FIGURE 2: The two photon coincidences as a function of time delay between detection events on the signal and idler arms exhibit a strong time correlation. The asymmetric shape of the correlation is a consequence of the time-ordered cascade decay. The observed $1/e$ decay time is shorter than the lifetime of the intermediate state, 27 ns due to collective effects in the atomic ensemble (superradiance).

Optical bandwidth and collective effects

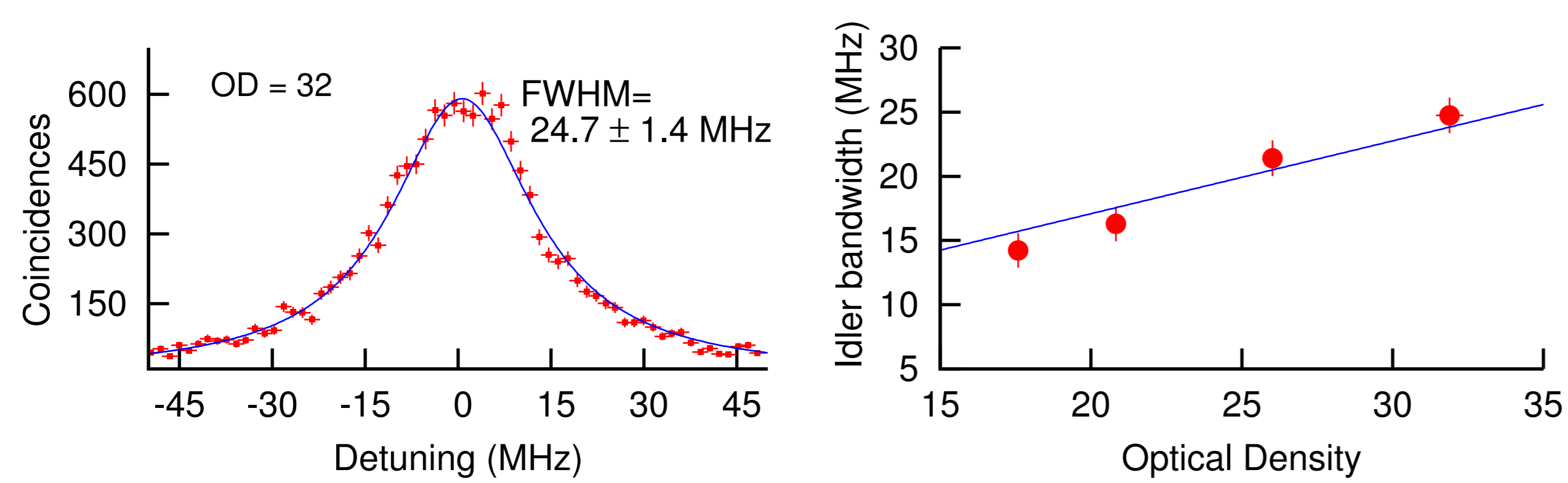


FIGURE 3: On the left, the spectral profile of idler photons, measured by scanning the Fabry-Pérot cavity and recording the coincidence rate for each detuning. The measured bandwidth matches the one expected by calculating the Fourier transform of the two-photon correlation function. On the right, we can observe how the optical density affects the idler bandwidth. The linear dependence is a signature of superradiance, as presented in [2].

Collinear setup

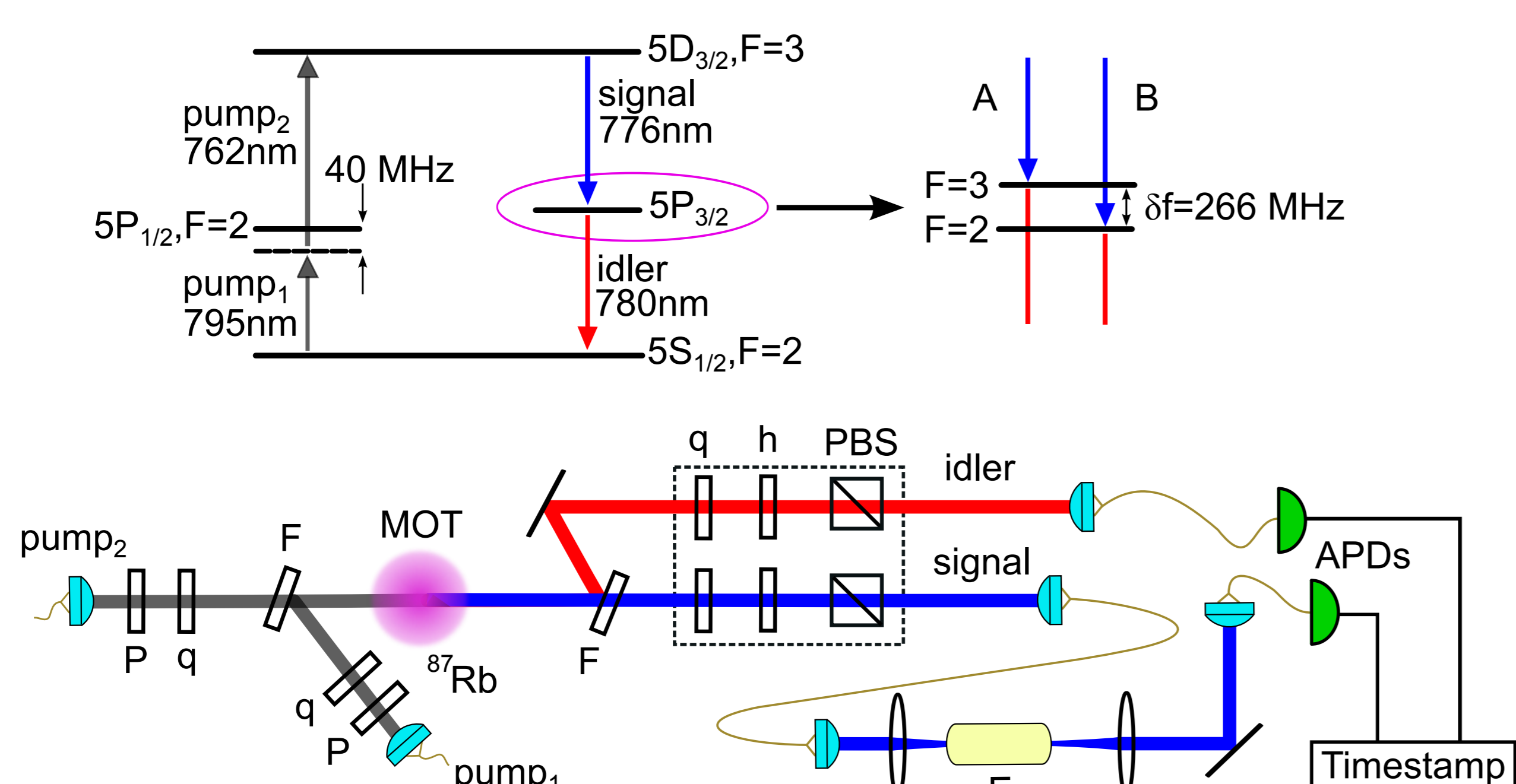


FIGURE 4: The source can also be used in a collinear geometry. Using a “reversed” level scheme, shown in the inset, the intermediate level offers two possible hyperfine levels contributing to the photon pair generation.

Biphoton state

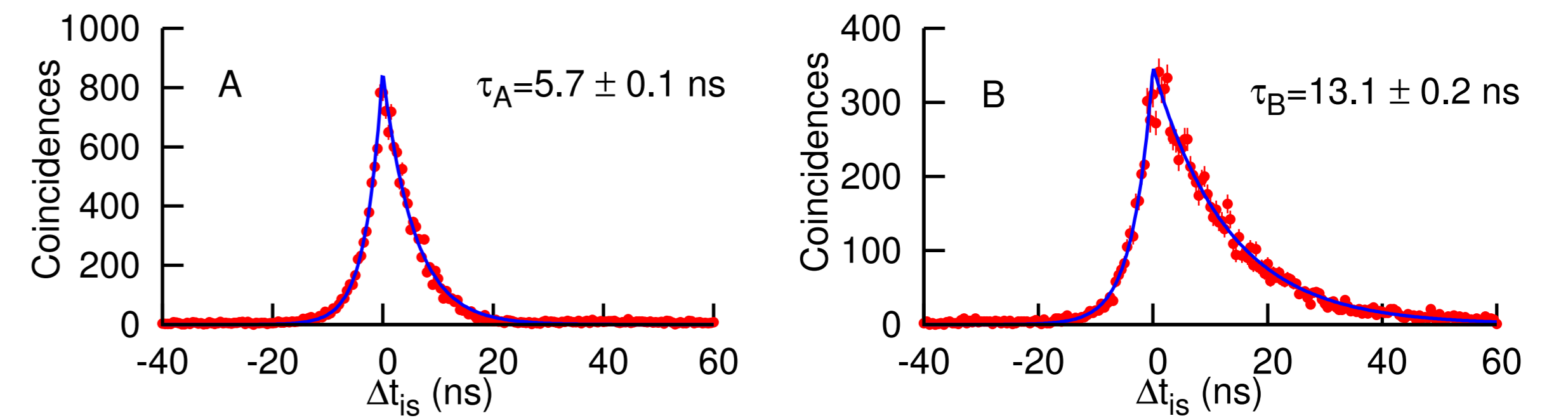


FIGURE 5: Time correlation of the generated biphoton for decays A (left) and B (right). The decay path is selected using a temperature tuned étalon. The transitions involved in decay A are stronger than those of decay B. This leads to a stronger collective effect in the atomic ensemble and hence faster decay. The rise time of 3.1 ns is due to finite bandwidth of the étalon.

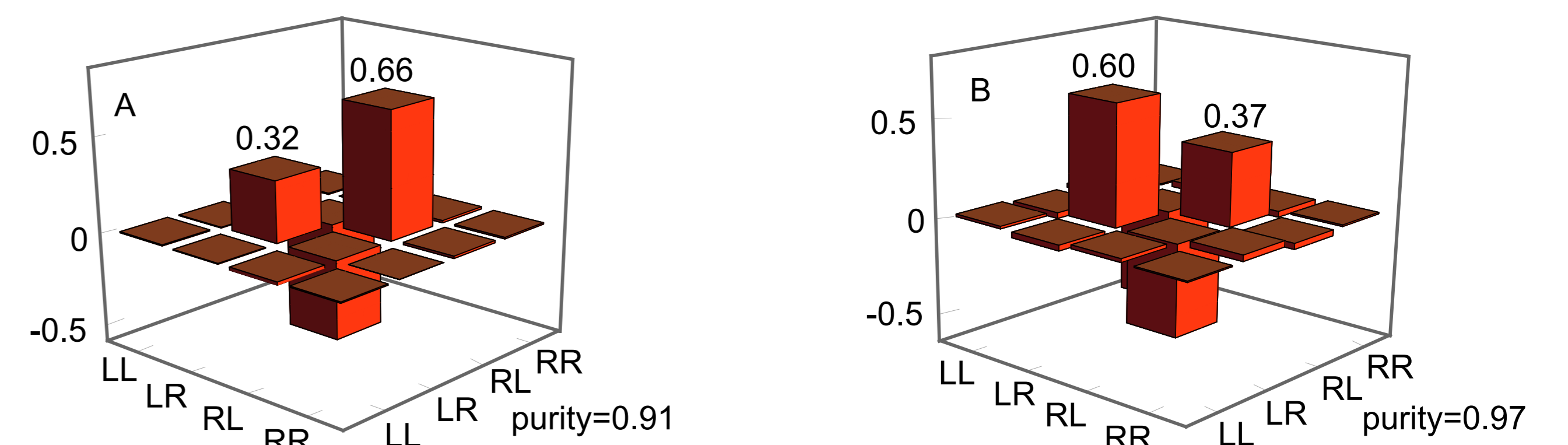


FIGURE 6: Tomographic reconstruction of the density matrix (real part only) for the biphotons generated via decay A (left) and B (right) with pumps set to orthogonal circular polarizations. The measured states are well approximated by the pure states $|\psi_A\rangle = 0.55|LR\rangle - 0.82|RL\rangle$, with a fidelity of 0.95, and $|\psi_B\rangle = 0.78|LR\rangle - 0.60|RL\rangle$, with a fidelity of 0.98.

Controlling quantum beats

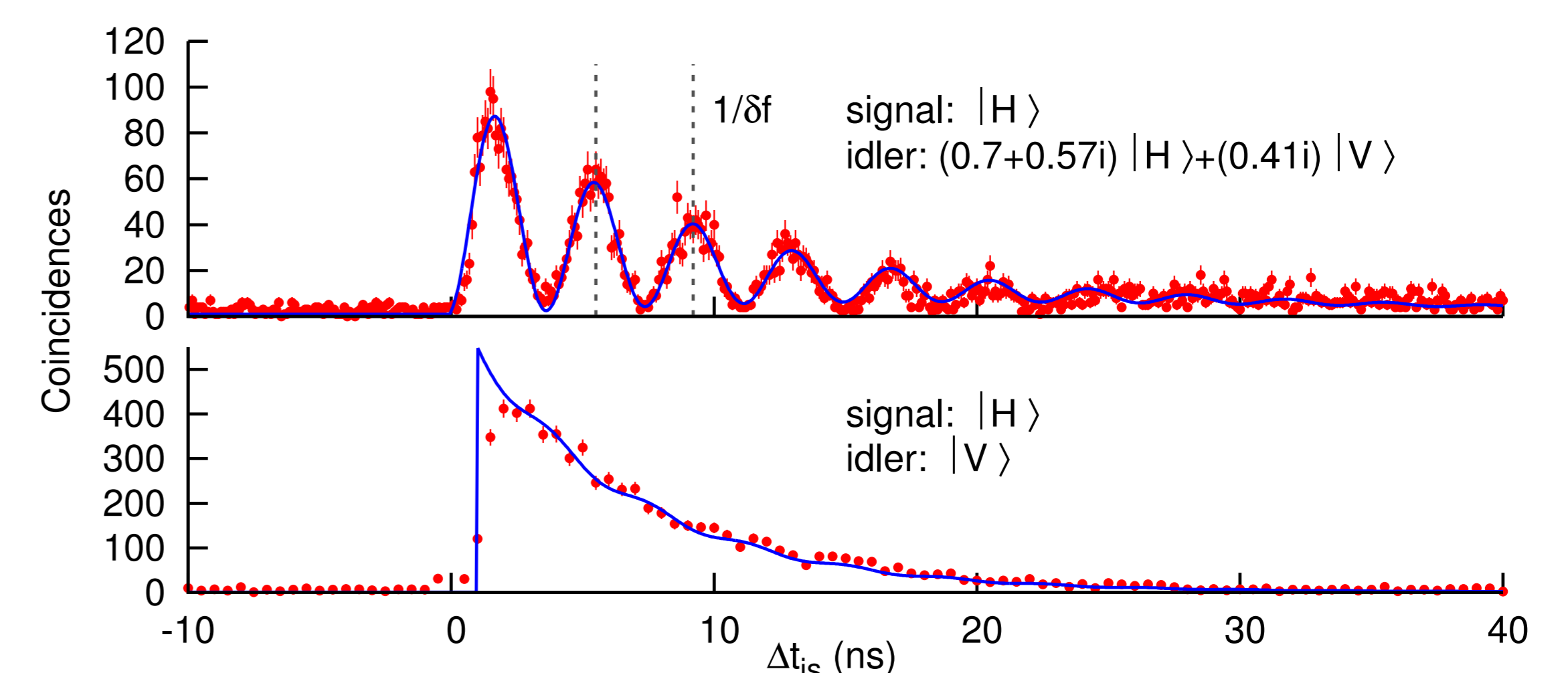


FIGURE 7: Without the étalon, the probability amplitude of decay paths A and B interfere, generating the oscillations shown in these graphs. This behavior is well described by a model based only on the Clebsch-Gordan coefficients of the transitions:

$$G_{is}^{(2)} = \Theta(\Delta t_{is}) \left[A^2 e^{-\frac{\Delta t_{is}}{\tau_A}} + B^2 e^{-\frac{\Delta t_{is}}{\tau_B}} + 2AB e^{-\frac{\Delta t_{is}}{2(\tau_A + \tau_B)}} \cos(2\pi \delta f \Delta t_{is} + \phi) \right],$$

where A and B are the relative strengths of the transitions and ϕ is their phase difference. The oscillations are then determined by the polarization of the pumps, signal, and idler modes.

In these measurements, the pumps are set to orthogonal linear polarizations. In the top plot, the visibility of the oscillation is maximized, reaching 94.1%. In the bottom one, we show how, choosing the appropriate polarizations, the oscillations can be damped, with the decay path B suppressed by a factor of 30.

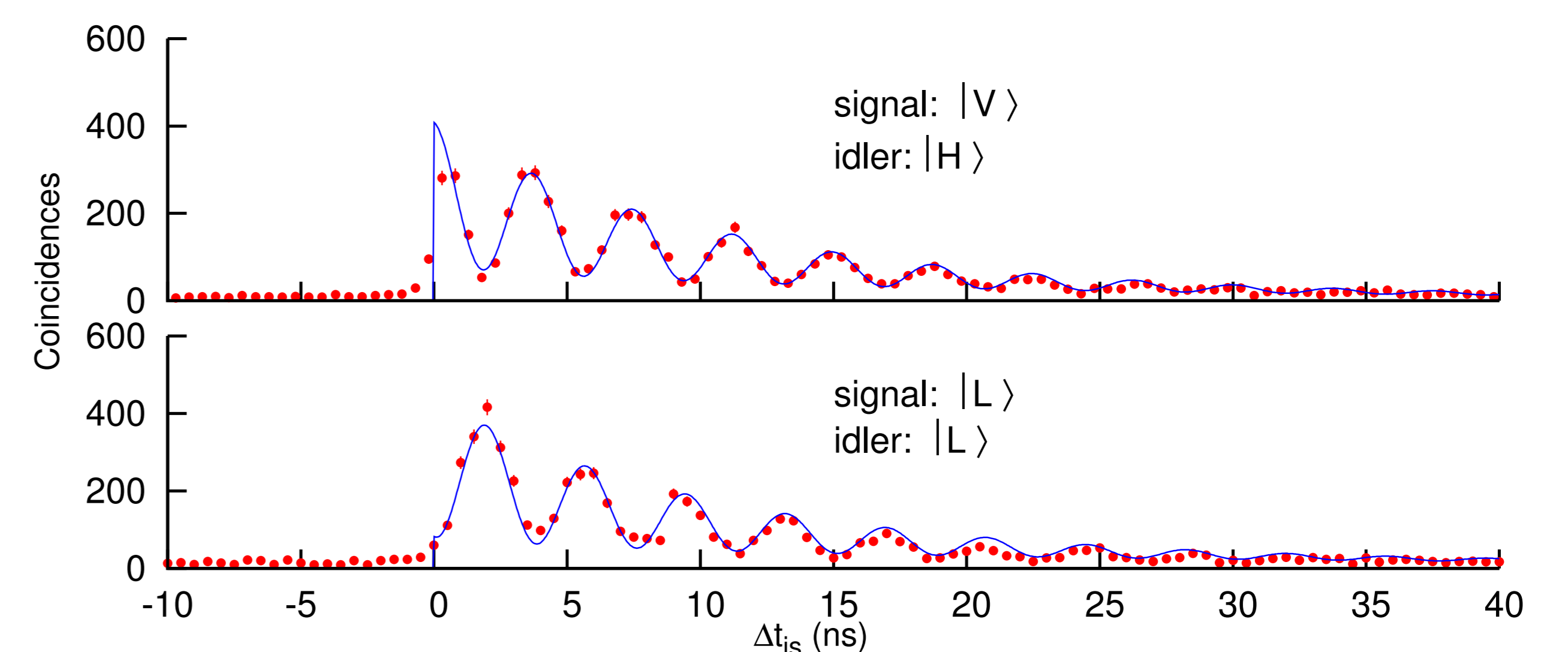


FIGURE 8: Similarly, the polarization projection allow us to control the phase of oscillation ϕ . In these two cases, the two oscillations have a phase difference of π .

Pair source performance

	762 – 795 nm pairs	776 – 780 nm pairs
Signal heralding efficiency	23 %	5 %
Idler heralding efficiency	19 %	10 %
Instantaneous pair rate	up to 18000 s^{-1}	up to 3000 s^{-1}
Bandwidth (FWHM)	8 – 25 MHz	10 – 32 MHz

References

- [1] T.Chaneliér et. al., Phys. Rev.Lett. 96, 093604 (2006).
- [2] B. Srivathsan et.al., Phys. Rev. Lett. 111, 123602 (2013).
- [3] G. K. Gulati, et.al. arXiv:1402.5800 (2014).